Sciencexpress Research Articles

Chelyabinsk Airburst, Damage Assessment, Meteorite Recovery, and Characterization

Olga P. Popova,[1] Peter Jenniskens,[2,3]* Vacheslav Emel'yanenko,[4] Anna Kartashova,[4] Eugeny Biryukov,[5] Sergey Khaibrakhmanov,[6] Valery Shuvalov,[1] Yurij Rybnov,[1] Alexandr Dudorov,[6] Victor I. Grokhovsky,[7] Dmitry D. Badyukov,[8] Qing-Zhu Yin,[9] Peter S. Gural,[2] Jim Albers,[2] Mikael Granvik,[10] Läslo G. Evers,[11,12] Jacob Kuiper,[11] Vladimir Kharlamov,[1] Andrey Solovyov,[13] Yuri S. Rusakov,[14] Stanislav Korotkiy,[15] Ilya Serdyuk,[16] Alexander V. Korochantsev,[8] Michail Yu Larionov,[7] Dmitry Glazachev,[1] Alexander E. Mayer,[6] Galen Gisler,[17] Sergei V. Gladkovsky,[18] Josh Wimpenny,[9] Matthew E. Sanborn,[9] Akane Yamakawa,[9] Kenneth L. Verosub,[9] Douglas J. Rowland,[19] Sarah Roeske,[9] Nicholas W. Botto,[9] Jon M. Friedrich,[20,21] Michael E. Zolensky,[22] Loan Le,[23,22] Daniel Ross,[23,22] Karen Ziegler,[24] Tomoki Nakamura,[25] Insu Ahn,[25] Jong Ik Lee,[26] Qin Zhou,[27,28] Xian-Hua Li,[28] Qiu-Li Li,[28] Yu Liu,[28] Guo-Qiang Tang,[28] Takahiro Hiroi,[29] Derek Sears,[3] Ilya A. Weinstein,[7] Alexander S. Vokhmintsev,[7] Alexei V. Ishchenko,[7] Phillipe Schmitt-Kopplin,[30,31] Norbert Hertkorn,[30] Keisuke Nagao,[32] Makiko K. Haba,[32] Mutsumi Komatsu,[33] Takashi Mikouchi[34] (the Chelyabinsk Airburst Consortium)

*Corresponding author. E-mail: Petrus.M.Jenniskens@nasa.gov

Author affiliatons are shown at the end of the text.

The asteroid impact near the Russian city of Chelyabinsk on 15 February 2013 was the largest airburst on Earth since the 1908 Tunguska event, causing a natural disaster in an area with a population exceeding one million. Because it occurred in an era with modern consumer electronics, field sensors, and laboratory techniques, unprecedented measurements were made of the impact event and the meteoroid that caused it. Here, we document the account of what happened, as understood now, using comprehensive data obtained from astronomy, planetary science, geophysics, meteorology, meteoritics, and cosmochemistry, and from social science surveys. A good understanding of the Chelyabinsk incident provides a unique opportunity to calibrate the event, with implications for the study of near-Earth objects and developing hazard mitigation strategies for planetary protection.

Chelyabinsk Oblast experienced an impact that was 100 times more energetic than the recent 4 kT of TNT equivalent Sutter's Mill (*1*). This was the biggest impact over land since the poorly observed Tunguska impact in 1908, for which kinetic energy estimates range from 3−5 (*2*) to 10−50 MT (*3*). From the measured period of infrasound waves circum traveling the globe (*4*), an early estimate of ~470 kT was derived for Chelyabinsk (*5*). Infrasound data from Russia and Kazakhstan provide 570 ± 150 kT; see supplementary materials (SM) Section 1.4 (*6*). Spaceborne visible and near-infrared observations (*7*) recorded a total irradiated energy of 90 kT (*5*, *8*), corresponding to a kinetic energy of 590 ± 50 kT using the calibration by Nemtchinov *et al*. (*9*). All values are uncertain by a factor of two because of a lack of calibration data at those high energies and altitudes.

The manner in which this kinetic energy was deposited in the atmosphere determined what shock wave reached the ground. Dash-cam and security camera videos of the fireball (Fig. 1) provide a lightcurve with peak brightness of -27.3 ± 0.5 magnitude (Fig. 2) (SM Sect. 1.2). The integrated lightcurve is consistent with other energy estimates if the panchromatic luminous efficiency was 7 ± 3%. Theoretical estimates under these conditions range from 5.6−13.2% (*10*).

Calibrated video observations provided a trajectory and pre-atmospheric orbit (Table 1) (SM Sect. 1.1). The fireball was first recorded at 97 km altitude, moving at 19.16 ± 0.15 km/s and entry angle 18.3 ± 0.2° with respect to the horizon, which is slightly faster than reported earlier (*11*). Combined with the best kinetic energy estimate, an entry mass of 1.3×10^7 kg (with a factor of two uncertainty) and a diameter of 19.8 ± 4.6 m is derived, assuming a spherical shape and the meteorite-derived density of 3.3 g/cm^3 based on x-ray computed tomography (SM Sect. 4.2, table S16).

Size and speed suggest that a shockwave first developed at 90 km. Observations show that dust formation and fragmentation started around 83 km and accelerated at 54 km (figs. S16 and S22). Peak radiation occurred at an altitude of 29.7 ± 0.7 km at 03:20:32.2 ± 0.1s UTC (SM Sect. 1.1-2), at which time spaceborne sensors measured a meteoroid speed of 18.6 km/s (*5*). Fragmentation left a thermally emitting debris cloud in this period, the final burst of which occurred at 27.0 km altitude (Fig. 1), with dust and gas settling at 26.2 km with distinctly higher billowing above that location (fig. S22). The dust cloud split in two due to buoyancy of the hot gas, leading to two cylindrical vortices (*12*).

Compared to the much larger Tunguska event (*2*, *3*), Chelyabinsk was only on the threshold of forming a common shock wave around the fragments when it broke at peak brightness (SM Sect. 1.2). Fragments were spatially isolated enough to be efficiently decelerated, avoiding the transfer of momentum to lower altitudes and resulting in less damage when the blast wave reached the ground.

Damage Assessment

In the weeks following the event, 50 villages were visited to verify the extent of glass damage. The resulting map (Fig. 3) demonstrates that the shockwave had a cylindrical component, extending furthest perpendicular to the trajectory. There was little coherence of the shockwave in the forward direction, where the disturbance was of long duration, shaking buildings and making people run outside, but causing no damage.

The strength of this shockwave on the ground was modeled (SM Sect. 2.4) assuming that an overpressure of $\Delta P > 500$ Pa was required (*13*). A 520 kT event, with detonations spread over altitudes ranging from 34−27 km and 24−19 km, would cause damage out to a distance of 120 km with the observed shape (Fig. 3). The fragments that penetrated

below 27 km must have contributed to the damage in order to match the shock wave arrival times (SM Sect. 2.4).

The number of houses damaged per 1,000 inhabitants (table S11) (SM Sect. 2.3) falls off with distance from the airburst source (r) as $r^{-2.6 \pm 1.2}$, with overpressure calculated to fall off as $r^{-2.4}$ (fig. S39). In Chelyabinsk itself, 3,613 apartment buildings (about 44%) had shattered and broken glass, but these were not evenly distributed in the city (fig. S37). Sharp sounds heard following the shockwave also point to the fragmentation causing a complicated distribution of pressure. Structural damage included the collapse of a zinc factory roof.

Directly below the fireball's path, the shock wave was strong enough to blow people off their feet. In Yemanzhelinsk, window frames facing the trajectory were pushed inwards, and suspended ceilings were sucked down above broken windows (fig. S36G). There was no structural damage to buildings, other than a statue of Pushkin inside the local library, cracked by a blown out window frame. Cracks in walls were documented in nearby Baturinsky and Kalachevo.

Electrophonic sounds were heard (SM Sect. 1.6), but there was no evidence of an Electromagnetic Pulse (EMP) under the track in neighboring Emanzhelinka. Due to shock wave induced vibrations, electricity and cell phone connectivity was briefly halted in the Kunashaksky district at the far northern end of the damage area. The gas supply was briefly interrupted in some districts due to valves reacting to the vibrations.

People found it painful to look at the bright fireball, but glancing away prevented lasting eye damage. Of 1,113 respondents to an internet survey who were outside at the time, 25 were sunburned (2.2%), 315 felt hot (28%) and 415 (37%) warm (SM Sect. 2.2). Mild sunburns were reported throughout the survey area (table S7), reflecting the fact that UV flux density falls off as $\sim r^{-2}$. In Korkino, 30 km from the point of peak brightness, one resident reported getting a mild sunburn on the face, followed by loss of skin flakes. Such effects occur at a minimum erythema dose of ~1,000 J/m^2 (*14*) of 290-320 nm radiation (mostly UV-B). Assuming 6,000 K radiation (*9*), the calculated dose would have been ~200 J/m^2 at Korkino. Ground-reflectance of UV light by snow may have further increased the dose.

Out of the total 1,674 collected internet queries, 374 mention 452 body injuries or inconveniences (SM Sect. 2.2). Of those, 5.3% reported sunburn, 48% eyes hurt, and 2.9% felt retinal burns. Because of the shock wave, 6.4% reported a concussion or mental confusion, upset, or exhaustion as a result of excessive stress. Flying glass and falling building debris affected a relatively small fraction of respondents: 4.8% reported cuts and 2.9% reported bruises, but no broken bones were reported.

The percentage of people asking for medical assistance (table S10) dropped with distance according to $r^{-3.2 \pm 0.5}$ (SM Sect. 2.1). The majority of injuries (1,210) took place in the densely populated Chelyabinsk city, but the highest fraction of people asking for assistance was near the trajectory track in the Korkinsky district (0.16%).

Meteorite Recovery

Shock radiation contributed to surface heating and ablation, but did not completely evaporate all fragments of Chelyabinsk, unlike in the case of Tunguska (*3*). Meteorites of ~0.1 g fell near Aleksandrovka close to the point of peak brightness, masses of ~100 g fell further along the trajectory near Deputatskiy, and at least one of 3.4 kg fell near Timiryazevskiy. One hit the roof of a house in Deputatskiy (fig. S46). Falling-sphere models suggest they originated at 32-26 km altitude (fig. S52), where the meteor model shows rapid fragmentation (fig. S18C). The location of the meteorites is consistent with prevailing NW winds of 5−15 m/s (fig. S24). An estimated 3,000−5,000 kg fell in this area (SM Sect. 3.1).

Two main fragments survived the disruption at 29.7 km. They flared around 24 km, with one falling apart at 18.5 km, and the other remaining luminous down to 13.6 km (Fig. 1 and fig. S15). Lightcurve modeling (SM Sect. 1.2) suggests that from this material another ~1 ton in larger fragments up to 100−400 kg in mass reached the ground. A 7-m sized hole was discovered in 70-cm thick ice on Lake Chebarkul (fig. S53A), in line with the trajectory (SM Sect. 1.1). A lakeshore video security camera, pointed to the site, recorded the impact (fig. S53B). Small meteorite fragments were recovered over an area up to 50 m from the impact location (Fig. 4C). Impact models (figs. S18 and S54) suggest a 200−1,000 kg meteorite would be required to create such a hole. A mass of ≥570 kg was recovered from the lakebed (fig. S53C).

The combined 4-6 t of surviving meteorites is only 0.03−0.05% of the initial mass. 76% of the meteoroid evaporated, with most of the remaining mass converted into dust (SM Sect. 1.3). Witnesses reported smelling "sulfur" and burning odors over a wide region concentrated near the fireball trajectory, starting about an hour after the fireball and lasting through much of the day (SM Sect. 1.5) (fig. S34).

Characterization of Recovered Meteorites

The unusually effective fragmentation and small surviving mass may have been caused by structural and material weakness. The asteroid had a lower compressive strength than the ~330 MPa measured for recovered, surviving meteorites (Section S4.1). The lightcurve (Fig. 2) is modeled with fragmentation starting at a low 0.2 MPa dynamic pressure, but tolerating higher pressure with decreasing fragment size. This is similar to other meteorite falls, where initial weakness was attributed to macroscopic cracks or microscopic porosity (*15*). For Chelyabinsk, however, the physical weakness is not microporosity related. X-ray computed tomography (SM Sect. 4.2) revealed a degree of compaction consistent with the lack of intragranular porosity typical of LL chondrites (*16*).

Some laboratory broken meteorites fragmented along shock veins (fig. S55), a possible weakness in the material that could have contributed to the abundant dust formation. The meteorite is composed of a breccia (*17*) of mildly shocked lighter clasts and moderately shocked darker clasts with abundant thin to cm-wide shock melt veins (Fig. 4A) (SM Sect. 4.4). A peculiar feature is that some shock veins exhibit a metal layer located ~20 microns inside the vein, which follows the outer contours of the vein (Fig. 4B), indicating that metal initially segregated from the most rapidly solidifying rims of the vein. This could contribute to weakness. Metal-rich tendrils also project outward from the vein.

The mineral compositional ranges (SM Sect. 4.4) are slightly larger than those reported before (*18*), but still compatible with a classification as LL5, shock stage S4 (*19*). The classification as LL chondrite is substantiated by oxygen and chromium isotope studies (SM Sect. 4.5−4.7), which put the meteorite near the L-end of the LL field (*20*, *21*) (Fig. 4D and fig. S68). Iron content and oxidation state also support the LL chondrite classification (Fig. 4E and fig. S58). Rare Earth element abundances are more similar to L chondrites (Fig. 4F and table S18), while one measured reflectance spectrum better matches that of H chondrites (fig. S72).

The Chelyabinsk (LL) parent body experienced a significant thermal and/or collision resetting event 115 ± 21 Ma after formation of the Solar System (*25*), not experienced by most other LL chondrites, possibly due to a significant impact event near its site of origin on the parent body. The phosphate U-Pb age is 4,452 ± 21 Ma (SM Sect. 4.8) (fig. S70), much younger than the majority of other ordinary chondrites phosphate ages dated by conventional TIMS methods (*22*, *23*). Perhaps one other piece of evidence for this is the 4.48 ± 0.12 Ga Pb-Pb isochron age of phosphates in a granite-like fragment found in the LL3-6 chondrite regolith breccia Adzhi-Bogdo (*24*), an observed fall in Mongolia in 1949.

Chelyabinsk shows a common orientation of metal grains indicating an impact-related petrofabric (fig. S59), stronger than that seen in any other ordinary chondrite of any shock stage (*26*) (fig. S60). This petro-

fabric probably reflects the most recent extraterrestrial shock event experienced by the Chelyabinsk meteoroid. The magnetic susceptibility value is at the upper end of the range for LL type (fig. S61) (*27*), closer to L type chondrites, suggestive of higher metal content in Chelyabinsk than a typical LL chondrite. However, detailed analysis of the remanent magnetization suggests that a shock event or the conditions of atmospheric entry led to significant resetting of the remanence (SM Sect. 4.3).

Recent meteoroid heating events are normally recorded by thermoluminescence (TL) (SM Sect. 4.10). In this case, the induced TL level of Chelyabinsk is lower than other petrographic type 5 or 6 chondrites, possibly because shock metamorphism to the level of S4 (30-35 GPa) (fig. S79) destroyed feldspar, the mineral phase responsible for the thermoluminescence signal (*28*). Atmospheric heating did not cause loss of natural TL signal, the steep thermal gradient being consistent with a very thin fusion crust on the measured samples (*29*). The natural TL value is consistent with the meteoroid having been heated at a perihelion distance of 0.6−0.8 AU (Table 1).

The shock did not remove all organic matter from the meteorite. Methanol-soluble polar organic compounds (Sect. S4.11) were detected in impact melt vein and chondrite fractions using electrospray ionization ion cyclotron resonance Fourier-Transform mass spectrometry (*30*). Out of more than 18,000 resolved mass peaks, 2,536 could be assigned to compounds containing C, H, N, O, S. The organic signature is typical of other shocked LL chondrites, showing a higher abundance of oxygen and nitrogen atoms in the impact melt (fig. S83). The presence of oxygenated sulfur is indicated by CHOS compounds containing on average 3 more oxygen atoms than CHO and CHNO compounds. The high abundance of CHOS compounds in a homologous series across the entire mass range testifies that most of these did not result from terrestrial contamination.

Impact shock induced fracturing on the Chelyabinsk parent body was followed by melting of metal and sulfides, which are pressure-driven through the meteorite. There are cases where this increased a meteorite's mechanical strength, the residual heat facilitating the process. However, in the case of Chelyabinsk, the production of cracks weakened the meteorite material more than shock melting increased its strength.

Source and Evolution of the Chelyabinsk Meteoroid

Chelyabinsk adds an LL5 type meteorite to a short list (SM Sect. 1.1) of 18 differently typed meteorites with known pre-atmospheric orbits (*1*). Only 8.2% of falls are LL chondrites (*31*). The Chelyabinsk meteorite is of particular interest because it is of the same type as asteroid Itokawa, from which samples were collected by the Hayabusa Mission (*32*). Indeed, both Itokawa and Chelyabinsk have similar low-inclined low-semi-major axis orbits (Table 1), which, according to one model (*33*), imply a 62%, 11%, and 25% probability for Chelyabinsk (and 71%, 0%, and 29% probability for Itokawa) of originating from the secular ν_6 resonance, the 3:1 mean-motion resonance, and the Intermediate Mars Crosser region, respectively. Multiplying these probabilities, assuming all LL chondrites enter the near Earth object region through the same escape route, there is now an 86% probability that they originated from ν_6. This supports the hypothesis (*34*) that they originated from the inner part of the LL-type (*35*) Flora asteroid family, which straddles the ν_6 resonance in 1.6−7.7° inclined orbits (*36*).

As a group, LL chondrites have a cosmic ray exposure age peaking at ~17 Ma (*34*). Chelyabinsk, on the other hand, was exposed only since ~1.2 Ma (SM Sect. 4.12). The responsible breakup that first exposed the Chelyabinsk meteoroid surface to cosmic rays was not likely part of the ongoing collision cascade in the asteroid main belt that followed the formation of the Flora family. Although fast pathways exist that can bring meteoroids from all three resonances into a Chelyabinsk-like orbit in about 0.2 Ma, such cases are rare (table S6). More likely, Chelyabinsk was exposed only since being ejected from the resonance, due to breakup from either thermal stresses, rotational spin-up, or from tidal forces in terrestrial planet encounters. The required structural weakness may have come from macroscopic cracks or from a weakly consolidated rubble pile morphology.

If tidal forces disrupted the Chelyabinsk meteoroid (*37*), events were set in motion 1.2 Ma ago during what was likely an earlier close encounter with Earth, when a 20-m sized chunk of subsurface Flora-family parent body rubble, rich in shock veins, separated from a larger object. The rest of that rubble could still be part of the near-Earth object population.

References and Notes

1. P. Jenniskens, M. D. Fries, Q. Z. Yin, M. Zolensky, A. N. Krot, S. A. Sandford, D. Sears, R. Beauford, D. S. Ebel, J. M. Friedrich, K. Nagashima, J. Wimpenny, A. Yamakawa, K. Nishiizumi, Y. Hamajima, M. W. Caffee, K. C. Welten, M. Laubenstein, A. M. Davis, S. B. Simon, P. R. Heck, E. D. Young, I. E. Kohl, M. H. Thiemens, M. H. Nunn, T. Mikouchi, K. Hagiya, K. Ohsumi, T. A. Cahill, J. A. Lawton, D. Barnes, A. Steele, P. Rochette, K. L. Verosub, J. Gattacceca, G. Cooper, D. P. Glavin, A. S. Burton, J. P. Dworkin, J. E. Elsila, S. Pizzarello, R. Ogliore, P. Schmitt-Kopplin, M. Harir, N. Hertkorn, A. Verchovsky, M. Grady, K. Nagao, R. Okazaki, H. Takechi, T. Hiroi, K. Smith, E. A. Silber, P. G. Brown, J. Albers, D. Klotz, M. Hankey, R. Matson, J. A. Fries, R. J. Walker, I. Puchtel, C. T. Lee, M. E. Erdman, G. R. Eppich, S. Roeske, Z. Gabelica, M. Lerche, M. Nuevo, B. Girten, S. P. Worden; Sutter's Mill Meteorite Consortium, Radar-enabled recovery of the Sutter's Mill meteorite, a carbonaceous chondrite regolith breccia. *Science* **338**, 1583–1587 (2012). doi:10.1126/science.1227163 Medline
2. M. B. E. Boslough, D. A. Crawford, Shoemaker-Levy 9 and Plume-forming collisions on Earth. *Ann. N. Y. Acad. Sci.* **822**, (1 Near-Earth Ob), 236–282 (1997). doi:10.1111/j.1749-6632.1997.tb48345.x
3. V. V. Svetsov, V. V. Shuvalov, Tunguska catastrophe of 30 June 1908, in *Catastrophic events Caused by Cosmic Objects*, V. Adushkin, I. Nemtchinov, Eds. (Springer, Dordrecht, 2008), pp. 227−267.
4. D. R. Christie, P. Campus, The IMS infrasound network: Design and establishment of infrasound stations, in *Infrasound Monitoring for Atmospheric Studies*, A. Le Pichon, E. Blanc, A. Hauchecorne, Eds. (Springer, Dordrecht 2010), pp. 29−75.
5. D. Yeomans, P. Chodas, Additional Details on the Large Fireball Event over Russia on Feb. 15, 2013. *NASA NEO Program Office Announcement, March 1, 2013* (NASA, Washington, 2013).
6. Materials and methods are available as supporting material on *Science* Online.
7. E. Tagliaferri, R. Spalding, C. Jacobs, S. P. Worden, A. Erlich, Detection of meteorite impacts by optical sensors in Earth orbit, in *Hazards Due to Comets and Asteroids, Space Science Series* (University of Arizona Press, Tucson, 1994), p. 199.
8. T. A. Ens, P. G. Brown, W. N. Edwards, E. A. Silber, Infrasound production of bolides: A global statistical study. *J. Atmos. Sol. Terr. Phys.* **80**, 208–229 (2012). doi:10.1016/j.jastp.2012.01.018
9. I. V. Nemtchinov, V. V. Svetsov, I. B. Kosarev, A. P. Golub', O. P. Popova, V. V. Shuvalov, R. E. Spalding, C. Jacobs, E. Tagliaferri, Assessment of kinetic energy of meteoroids detected by satellites-based light sensors. *Icarus* **130**, 259–274 (1997). doi:10.1006/icar.1997.5821
10. D. O. Revelle, Z. Ceplecha, Bolide physical theory with application to PN and EN fireballs. *ESA Special Publ.* **495**, 507–512 (2001).
11. J. Borovicka, P. Spurny, L. Shrbeny, Trajectory and orbit of the Chelyabinsk superbolide. CBET 3423, IAU Central Bureau for Astronomical Telegrams, D. W. E. Green, Ed., p. 1−1 (2013).
12. J. Zinn, J. Drummond, Observations of persistent Leonid meteor trails: 4. Buoyant rise/vortex formation as mechanism for creation of parallel meteor train pairs. *JGR Space Physics* **110**, (A4), A04306 (2005). doi:10.1029/2004JA010575
13. S. Glasstone, P. J. Dolan, *The Effects of Nuclear Weapons, Third edition* (U.S. Government Printing Office, Washington, D.C. (1977), 1−174.
14. M.-W. Huang, P.-Y. Lo, K.-S. Cheng, Objective assessment of sunburn and minimal erythema doses: Comparison of noninvasive in vitro measuring techniques after UVB irradiation. *EURASIP J. Adv. Signal Process.* **2010**, 483562 (2010). doi:10.1155/2010/483562

15. O. Popova, J. Borovicka, W. K. Hartmann, P. Spurny, E. Gnos, I. Nemtchinov, J. M. Trigo-Rodríguez, Very low strengths of interplanetary meteoroids and small asteroids. *Meteorit. Planet. Sci.* **46**, 1525–1550 (2011). doi:10.1111/j.1945-5100.2011.01247.x
16. G. J. Consolmagno, D. T. Britt, R. J. Macke, The significance of meteorite density and porosity. *Chem. Erde* **68**, 1–29 (2008). doi:10.1016/j.chemer.2008.01.003
17. A. Bischoff, E. R. D. Scott, K. Metzler, C. A. Goodrich, Nature and origins of meteoric breccias, in *Meteorites and the Early Solar System II*, D. S. Lauretta, H. Y. McSween Jr., Eds. (University of Arizona Press, Tucson, AZ, 2006), pp. 679−712.
18. M. A. Nazarov, D. D. Badyukov, N. N. Kononkova, I. V. Kubrakova, Chelyabinsk Meteoritical Bulletin: Entry for Chelyabinsk; http://www.lpi.usra.edu/meteor/metbull.php?code=57165 (2013).
19. D. Stöffler, K. Keil, E. R. D. Scott, Shock metamorphism of ordinary chondrites. *Geochim. Cosmochim. Acta* **55**, 3845–3867 (1991). doi:10.1016/0016-7037(91)90078-J
20. R. N. Clayton, T. K. Mayeda, J. N. Goswami, E. J. Olsen, Oxygen isotope studies of ordinary chondrites. *Geochim. Cosmochim. Acta* **55**, 2317–2337 (1991). doi:10.1016/0016-7037(91)90107-G
21. A. Trinquier, J.-L. Birck, C. J. Allègre, Widespread ^{54}Cr Heterogeneity in the Inner Solar System. *Astrophys. J.* **655**, 1179–1185 (2007). doi:10.1086/510360
22. C. Göpel, G. Manhès, C. J. Allègre, U-Pb systematics of phosphates from equilibrated ordinary chondrites. *Earth Planet. Sci. Lett.* **121**, 153–171 (1994). doi:10.1016/0012-821X(94)90038-8
23. Y. Amelin, Meteorite phosphates show constant ^{176}Lu decay rate since 4557 million years ago. *Science* **310**, 839–841 (2005). doi:10.1126/science.1117919 Medline
24. K. Terada, A. Bischoff, Asteroidal granite-like magmatism 4.53 Gyr ago. *Astrophys. J.* **699**, L68–L71 (2009). doi:10.1088/0004-637X/699/2/L68
25. J. N. Connelly, M. Bizzarro, A. N. Krot, Å. Nordlund, D. Wielandt, M. A. Ivanova, The absolute chronology and thermal processing of solids in the solar protoplanetary disk. *Science* **338**, 651–655 (2012). doi:10.1126/science.1226919 Medline
26. J. M. Friedrich, J. C. Bridges, M.-S. Wang, M. E. Lipschutz, Chemical studies of L chondrites. VI: Variations with petrographic type and shock-loading among equilibrated falls. *Geochim. Cosmochim. Acta* **68**, 2889–2904 (2004). doi:10.1016/j.gca.2004.01.010
27. P. Rochette, L. Sagnotti, M. Bourout-Denise, G. Consolmagno, L. Folco, J. Gattacceca, M. L. Osete, L. Pesonen, Magnetic classification of stony meteorites: 1. Ordinary chondrites. *Meteorit. Planet. Sci.* **38**, 251–268 (2003). doi:10.1111/j.1945-5100.2003.tb00263.x
28. C. P. Hartmetz, D. W. G. Sears, Thermoluminescence properties of shocked and annealed plagioclases with implications for meteorites. *Meteoritics* **22**, 400–401 (1988).
29. D. W. Sears, A. A. Mills, Temperature gradients and atmospheric ablation rates for the Barwell meteorite. *Nat. Phys. Sci (Lond.)* **242**, 25–26 (1973). doi:10.1038/physci242025a0
30. P. Schmitt-Kopplin, Z. Gabelica, R. D. Gougeon, A. Fekete, B. Kanawati, M. Harir, I. Gebefuegi, G. Eckel, N. Hertkorn, High molecular diversity of extraterrestrial organic matter in Murchison meteorite revealed 40 years after its fall. *Proc. Natl. Acad. Sci. U.S.A.* **107**, 2763–2768 (2010). doi:10.1073/pnas.0912157107 Medline
31. T. L. Dunn, T. H. Burbine, W. F. Bottke, Jr., J. P. Clark, Mineralogies and source regions of near Earth asteroids. *Icarus* **222**, 273–282 (2013). doi:10.1016/j.icarus.2012.11.007
32. T. Nakamura, T. Noguchi, M. Tanaka, M. E. Zolensky, M. Kimura, A. Tsuchiyama, A. Nakato, T. Ogami, H. Ishida, M. Uesugi, T. Yada, K. Shirai, A. Fujimura, R. Okazaki, S. A. Sandford, Y. Ishibashi, M. Abe, T. Okada, M. Ueno, T. Mukai, M. Yoshikawa, J. Kawaguchi, Itokawa dust particles: A direct link between S-type asteroids and ordinary chondrites. *Science* **333**, 1113–1116 (2011). doi:10.1126/science.1207758 Medline
33. W. F. Bottke, A. Morbidelli, R. Jedicke, J.-M. Petit, H. F. Levison, P. Michel, T. S. Metcalfe, De-biased orbital and absolute magnitude distributions of Near Earth Objects. *Icarus* **156**, 339–433 (2000).
34. P. Michel, M. Yoshikawa, Dynamical origin of the asteroid (25143) Itokawa: The target of the sample-return Hayabusa space mission. *Astron. Astrophys.* **449**, 817–820 (2006). doi:10.1051/0004-6361:20054319
35. V. Reddy, J. M. Carvano, D. Lazzaro, T. A. Michtchenko, M. J. Gaffey, M. S. Kelley, T. Mothé-Diniz, A. Alvarez-Candal, N. A. Moskovitz, E. A. Cloutis, E. L. Ryan, Mineralogical characterization of Baptistina Asteroid Family: Implications for K/T impactor source. *Icarus* **216**, 184–197 (2011). doi:10.1016/j.icarus.2011.08.027
36. D. Nesvorny, A. Morbidelli, D. Vokrouhlicky, W. F. Bottke, M. Broz, The Flora family: A case of the dynamically dispersed collisional swarm? *Icarus* **157**, 155–172 (2002). doi:10.1006/icar.2002.6830
37. E. Schunová, M. Granvik, R. Jedicke, G. Gronchi, R. Wainscoat, S. Abe, Searching for the first near-Earth object family. *Icarus* **220**, 1050–1063 (2012). doi:10.1016/j.icarus.2012.06.042
38. J. Troiano, D. Rumble, III, M. L. Rivers, J. M. Friedrich, Compositions of three low-FeO ordinary chondrites: indications of a common origin with the H chondrites. *Geochim. Cosmochim. Acta* **75**, 6511–6519 (2011). doi:10.1016/j.gca.2011.08.033
39. W. F. McDonough, Compositional model for the Earth's core, in *The Mantle and Core, Vol. 2. Treatise on Geochemistry*, R. W. Carlson, Ed. (Elsevier-Pergamon, Oxford, 2003), 547–568.
40. J. T. Wasson, G. W. Kallemeyn, Compositions of chondrites. *Phil. Trans. Roy. Soc. London A* **325**, 535–544 (1988). doi:10.1098/rsta.1988.0066
41. J. M. Friedrich, M.-S. Wang, M. E. Lipschutz, Chemical studies of L chondrites. V: Compositional patterns for 49 trace elements in 14 L4-6 and 7 LL4-6 Falls. *Geochim. Cosmochim. Acta* **67**, 2467–2479 (2003). doi:10.1016/S0016-7037(03)00024-3
42. J. I. Zuluaga, I. Ferrin, A preliminary reconstruction of the orbit of the Chelyabinsk meteoroid. 21 Feb 2013, arXiv:1302.5377v1 [astro-ph.ED] (2013).
43. P. Jenniskens, P. S. Gural, L. Dynneson, B. J. Grigsby, K. E. Newman, M. Borden, M. Koop, D. Holman, CAMS: Cameras for allsky meteor surveillance to establish minor meteor showers. *Icarus* **216**, 40–61 (2011). doi:10.1016/j.icarus.2011.08.012
44. P. S. Gural, A new method of meteor trajectory determination applied to mulitple unsynchronized video cameras. *Meteorit. Planet. Sci.* **47**, 1405–1418 (2012). doi:10.1111/j.1945-5100.2012.01402.x
45. F. L. Whipple, L. G. Jacchia, Reduction methods for photographic meteor trails. *Smiths. Contr. Astrophysics* **1**, 183–206 (1957). doi:10.5479/si.00810231.1-2.183
46. J. Borovicka, P. Spurny, L. Shrbeny, Trajectory and orbit of the Chelyabinsk superbolide. CBET 3423, D. W. E. Green, Ed., *Central Bureau for Astronomical Telegrams, International Astronomical Union*, p. 1–1 (2013).
47. D. Yeomans, P. Chodas, Additional details on the large fireball event over Russia on Feb. 15, 2013. NASA/JPL Near-Earth Object Program Office, March 1, 2013; http://neo.jpl.nasa.gov/news/fireball_130301.html (2013).
48. B. J. Gladman, F. Migliorini, A. Morbidelli, V. Zappala, P. Michel, A. Cellino, C. Froschle, H. F. Levison, M. Bailey, M. Duncan, Dynamical lifetimes of objects injected into asteroid belt. *Science* **277**, 197–201 (1997). doi:10.1126/science.277.5323.197
49. P. Jenniskens, Observations of the Stardust Sample Return Capsule entry with a slitless echelle spectrograph. *J. Spacecr. Rockets* **47**, 718–735 (2010). doi:10.2514/1.37518
50. O. Popova, Meteoroid ablation models. *Earth Moon Planets* **95**, 303–319 (2004). doi:10.1007/s11038-005-9026-x
51. V. V. Svetsov, I. V. Nemtchinov, A. V. Teterev, Disintegration of large meteoroids in Earth's atmosphere: Theoretical models. *Icarus* **116**, 131–153 (1995). doi:10.1006/icar.1995.1116
52. A. P. Golub', I. B. Kosarev, I. V. Nemtchinov, O. P. Popova, Emission spectra of bright bolides. *Sol. Syst. Res.* **31**, 85–98 (1997).
53. M. Boslough, D. Crawford, A. Robinson, T. Trucano, Mass and penetration depth of Shoemaker-Levy 9 fragments from time-resolved photometry. *Geophys. Res. Lett.* **21**, 1555–1558 (1994). doi:10.1029/94GL01582
54. V. V. Shuvalov, N. A. Artemieva, Numerical modeling of Tunguska-like impacts. *Planet. Space Sci.* **50**, 181–192 (2002). doi:10.1016/S0032-0633(01)00079-4
55. B. Baldwin, Y. Sheaffer, Ablation and breakup of large meteoroids during atmospheric entry. *J. Geophys. Res.* **76**, 4653–4668 (1971). doi:10.1029/JA076i019p04653
56. J. Borovička, O. P. Popova, I. V. Nemtchinov, P. Spurný, Z. Ceplecha, Bolides produced by impacts of large meteoroids into the Earth's atmosphere: Comparison of theory with observations. I. Benesov bolide dynamics and

fragmentation. *Astron. Astrophys.* **334**, 713–728 (1998).
57. P. A. Bland, N. A. Artemieva, The rate of small impacts on Earth. *Meteorit. Planet. Sci.* **41**, 607–631 (2006). doi:10.1111/j.1945-5100.2006.tb00485.x
58. Z. Ceplecha, P. Spurny, J. Borovička, J. Keclikova, Atmospheric fragmentation of meteoroids. *Astron. Astrophys.* **279**, 615–626 (1993).
59. Z. Ceplecha, D. O. Revelle, Fragmentation model of meteoroid motion, mass loss, and radiation in the atmosphere. *Meteorit. Planet. Sci.* **40**, 35–54 (2005). doi:10.1111/j.1945-5100.2005.tb00363.x
60. O. P. Popova, Passage of Bolides Through the Atmosphere. Meteoroids: The Smallest Solar System Bodies, Proc. Meteoroids Conference, Breckenridge, Colorado, USA, May 24–28, 2010, W. J. Cooke, D. E. Moser, B. F. Hardin, D. Janches, Eds. NASA/CP-2011-216469, p. 232 (2011).
61. V. I. Tsvetkov, A. Ya. Skripnik, Atmospheric fragmentation of meteorites according to strength theory. *Sol. Syst. Res.* **25**, 273–279 (1991).
62. O. Popova, J. Borovička, W. K. Hartmann, P. Spurný, E. Gnos, I. Nemtchinov, J. M. Trigo-Rodríguez, Very low strength of interplanetary meteoroids and small asteroids. *Meteorit. Planet. Sci.* **46**, 1525–1550 (2011). doi:10.1111/j.1945-5100.2011.01247.x
63. Z. Ceplecha, J. Borovička, W. G. Elford, D. O. ReVelle, R. L. Hawkes, V. Í. Porubčan, M. Šimek, Meteor phenomena and bodies. *Space Sci. Rev.* **84**, 327–471 (1998). doi:10.1023/A:1005069928850
64. A. P. Golub', I. B. Kosarev, I. V. Nemtchinov, V. V. Shuvalov, Emission and ablation of a large meteoroid in the course of its motion through the Earth's atmosphere. *Sol. Syst. Res.* **30**, 183–197 (1996).
65. I. V. Nemtchinov, V. V. Svetsov *et al*., Assessment of kinetic energy of meteoroids detected by satellite-based light sensors. *Icarus* **130**, 259–274 (1997). doi:10.1006/icar.1997.5821
66. A. R. Klekociuk, P. G. Brown, D. W. Pack, D. O. ReVelle, W. N. Edwards, R. E. Spalding, E. Tagliaferri, B. B. Yoo, J. Zagari, Meteoritic dust from the atmospheric disintegration of a large meteoroid. *Nature* **436**, 1132–1135 (2005). doi:10.1038/nature03881 Medline
67. J. Borovička, Z. Charavat, Meteosat observation of the atmospheric entry of 2008 TC3 over Sudan and associated dust cloud. *Astron. Astrophys.* **507**, 1015–1022 (2009). doi:10.1051/0004-6361/200912639
68. J. Zinn, J. Drummond, Observations of persistent Leonid meteor trails: 4. Buoyant model rise/vortex formation as mechanism for creation of parallel meteor train pairs. *JGR Space Physics* **110**, (A4), A04306 (2005). doi:10.1029/2004JA010575
69. Comprehensive Nuclear-Test-Ban Treaty organization (CTBTO) press release, 18.02.2013; http://www.ctbto.org/press-centre/press-releases/2013/russian-fireball-largest-ever-detected-by-ctbtos-infrasound-sensors/ (2013).
70. Y. Cansi, An automatic seismic event processing for detection and location: The P.M.C.C. method. *Geophys. Res. Lett.* **22**, 1021–1024 (1995). doi:10.1029/95GL00468
71. Yu. S. Rybnov, V. A. Kharlamov, V. F. Evmenov, Infrasound registration system of acoustic-gravitational waves, in *Dynamic Processes in a System of Inner and Outer Interacting Geospheres*, V. V. Adushkin, Ed., pp. 29–34 (2005).
72. M. A. Tsikulin, Shock waves during the movement of large meteorites in the atmosphere. Moscow, Nauka, 86 p. (1969). (English Translation: AD 715-537, National Technical Information Service, Springfield, Virginia, 1970)
73. D. O. ReVelle, Historical detection of atmospheric impacts by large bolides using acoustic-gravity waves, in Annals of the New York Academy of Sciences, Near- Earth Objects: The United Nations International Conference, J. L. Remo, Ed., New York Academy of Sciences, 822, 284–302 (1997).
74. W. N. Edwards, P. G. Brown, D. O. ReVelle, Estimates of meteoroid kinetic energies from observations of infrasonic airwaves. *J. Atmos. Sol. Terr. Phys.* **68**, 1136–1160 (2006). doi:10.1016/j.jastp.2006.02.010
75. W. N. Edwards, Meteor generated infrasound: Theory and observation, in *Infrasound Monitoring for Atmospheric Studies*, A. Le Pichon, E. Blanc, A. Hauchecorne, Eds., (Springer, Dordrecht, Netherlands, 2010), pp. 361–414.
76. E. Silber, D. O. ReVelle, P. G. Brown, W. N. Edwards, An estimate of the terrestrial influx of large meteoroids from infrasonic measurements. *J. Geophys. Res.* **114**, (E8), E08006 (2009). doi:10.1029/2009JE003334
77. J. L. Stevens, D. A. Adams, G. E. Baker, H. Xu, J. R. Murphy, I. Divnov, V. N. Bourchik, Infrasound Modeling Using Soviet Explosion Data and Instrument Design Criteria from Experiments and Simulations. Technical Report ADA446517S (2006).
78. P. Brown, A preliminary report on the Chelyabinsk fireball/airburst. *J. Int. Meteor Org.* **41**, 22–25 (2013).
79. J. P. Mutschlecner, R. W. Whitaker, L. H. Auer, An empirical study of infrasonic propagation, Los Alamos National Laboratory Technical Report, LA-13620-MS, Los Alamos, NM (1999).
80. J. P. Mutschlecner, R. W. Whitaker, Some atmospheric effects on infrasound signal amplitudes, in *Infrasound Monitoring for Atmospheric Studies*, A. Le Pichon, E. Blanc, A. Hauchecorne, Eds. (Springer, Dordrecht, Netherlands, 2010), pp. 455–474.
81. K. E. Gubkin, About similarity of explosions. *Физ. Земли Fizika Zemli* **N10**, 49–60 (1978).
82. J. Reed, Airblast overpressure decay at long ranges. *J. Geophys. Res.* **77**, 1623–1629 (1972). doi:10.1029/JC077i009p01623
83. V. N. Arkhipov *et al*., Mechanical Action of Nuclear Explosions. (Fizmatlit, Moscow, (2003), 384 p.
84. S. Glasstone, P. J. Dolan, *The Effects of Nuclear Weapons* (U.S. Department of Defense, U.S. Department of Energy, Washington, 1977).
85. J. Reed, Climatology of Airblast Propagations from Nevada Test Site Nuclear Airbursts. Sandia Laboratories Report SC-RR-69-572 (1969).
86. M. Lutzky, D. Lechto, Shock propagation in spherically symmetric exponential atmosphere. *Phys. Fluids* **11**, 1466–1472 (1968). doi:10.1063/1.1692129
87. S. Mannan, F. P. Lees, Lees' Loss Prevention in the Process Industries: Hazard Identification, Assessment and Control, vol. 1, 3rd edition (Elsevier Butterworth-Heinemann, 2005).
88. M. D. Brown, A. S. Loewe, Reference manual to mitigate potential terrorist attacks against buildings. USA, FEMA, p. 4–19 (2003).
89. V. V. Shuvalov, Multi-dimensional hydrodynamic code SOVA for interfacial flows: Application to thermal layer effect. *Shock Waves* **9**, 381–390 (1999). doi:10.1007/s001930050168
90. N. M. Kuznetsov, Thermodynamic Functions and Shock Adiabats for Air at high Temperatures (Mashinostroyenie, Moscow, 1965).
91. C. E. Needham, *Blast Waves: Shock Wave And High Pressure Phenomena* (Springer-Verlag, Berlin, 2010), 339 pp..
92. J. R. Blackford, Sintering and microstructure of ice: A review. *J. Phys. D.* **40**, R355–R385 (2007). doi:10.1088/0022-3727/40/21/R02
93. A. van Herwijnen, D. A. Miller, Experimental and numerical investigation of the sintering of snow. *J. Glaciol.* **59**, 269–274 (2013). doi:10.3189/2013JoG12J094
94. A. N. Kolmogorov, Selected Proceedings: Probability Theory and Mathematical Statistics, M. Nauka, Ed. (1986).
95. I. T. Zotkin, Stony meteorite shower Tsarev. *Meteoritika* **41**, 3–12 (1982).
96. P. Jenniskens, M. H. Shaddad, D. Numan, S. Elsir, A. M. Kudoda, M. E. Zolensky, L. Le, G. A. Robinson, J. M. Friedrich, D. Rumble, A. Steele, S. R. Chesley, A. Fitzsimmons, S. Duddy, H. H. Hsieh, G. Ramsay, P. G. Brown, W. N. Edwards, E. Tagliaferri, M. B. Boslough, R. E. Spalding, R. Dantowitz, M. Kozubal, P. Pravec, J. Borovicka, Z. Charvat, J. Vaubaillon, J. Kuiper, J. Albers, J. L. Bishop, R. L. Mancinelli, S. A. Sandford, S. N. Milam, M. Nuevo, S. P. Worden, The impact and recovery of asteroid 2008 TC(3). *Nature* **458**, 485–488 (2009). doi:10.1038/nature07920 Medline
97. Q. R. Passey, H. J. Melosh; Q. R. Passey H. J. Melosh, Effects of atmospheric breakup on crater field formation. *Icarus* **42**, 211–233 (1980). doi:10.1016/0019-1035(80)90072-X
98. E. D. Narkhov, V. A. Sapunov, A. Yu. Denisov, D. V. Savelyev, D. A. Galkin, D. S. Yakovenko, A. L. Fedorov, Magnetic prospecting and data interpretation of the Chebarkul meteorite. In: Proceedings of the International Workshop Asteroids and Comets: The Chelyabinsk event and the Chebarkul lake meteorite fall, Chebarkul, June 21–22, 2013, (Kray Ra, Chelyabinsk, 2013), pp. 72–75.
99. M. L. Gittings *et al*., The RAGE radiation-hydrodynamic code, Los Alamos National Laboratory Report LA-UR- 06-0027, Los Alamos, New Mexico. Published in: Computational Science and Discovery 1, 015005 (2008).
100. J. Kimberley, K. T. Ramesh, The dynamic strength of an ordinary chondrite. Meteoritics and Plan. *Sci.* **46**, 1653–1669 (2011).
101. R. V. Medvedev, F. Gorbachevich, I. Zotkin, Determination of physical properties of stone meteorites from the point of view of their disruption. *Meteoritika* **44**, 105–110 (1985).
102. I. T. Zotkin, P. V. Medvedev, F. F. Gorbatsevich, Strength properties of the Tsarev meteorite. *Meteoritika* **46**, 86–93 (1987).

103. E. N. Slyuta, S. M. Nikitin, A. V. Korochantsev, C. A. Lorents, A. Ya. Skripnik, Strong physical and mechanical anisotropy of ordinary chondrites. 40th Lunar and Planetary Science Conference, Abstr.1051 (2010).
104. J. M. Friedrich, Quantitative methods for three-dimensional comparison and petrographic description of chondrites. *Comput. Geosci.* **34**, 1926–1935 (2008). doi:10.1016/j.cageo.2008.05.001
105. J. M. Friedrich, D. P. Wignarajah, S. Chaudhary, M. L. Rivers, C. E. Nehru, D. S. Ebel, Three-dimensional petrography of metal phases in equilibrated L chondrites: Effects of shock loading and dynamic compaction. *Earth Planet. Sci. Lett.* **275**, 172–180 (2008). doi:10.1016/j.epsl.2008.08.024
106. E. Jarosewich, Chemical analyses of meteorites: A compilation of stony and iron meteorite analyses. *Meteoritics* **25**, 323–337 (1990). doi:10.1111/j.1945-5100.1990.tb00717.x
107. H. C. Urey, H. Craig, The composition of the stone meteorites and the origin of the meteorites. *Geochim. Cosmochim. Acta* **4**, 36–82 (1953). doi:10.1016/0016-7037(53)90064-7
108. A. J. Brearley, R. H. Jones, Chondritic meteorites, in *Planetary Materials*, J. J. Papike, Ed., Mineralogical Society of America, Reviews in Mineralogy 36, pp. 3-1–3-398 (1998).
109. A. N. Krot, K. Keil, E. R. D. Scott, C. A. Goodrich, M. K. Weisberg, Classification of meteorites and their genetic relationships, in *Meteorites, Comets and Planets*, A. M. Davis, Ed., Vol. 1, Treatise on Geochemistry (K. K. Turekian, H. D. Holland, Eds.) (Elsevier, Oxford, 2013).
110. J. M. Friedrich, A. Ruzicka, M. L. Rivers, D. S. Ebel, J. O. Thostenson, R. A. Rudolph, Metal veins in the Kernouve (H6 S1) chondrite: Evidence for pre- or syn-metamorphic shear deformation. *Geochim. Cosmochim. Acta* **116**, 71–83 (2013). doi:10.1016/j.gca.2013.01.009
111. N. H. Woodcock, Specification of fabric shapes using an eigenvalue method. *Geol. Soc. Am. Bull.* **88**, 1231–1236 (1977). doi:10.1130/0016-7606(1977)88<1231:SOFSUA>2.0.CO;2
112. N. H. Woodcock, M. A. Naylor, Randomness testing in three-dimensional orientation data. *J. Struct. Geol.* **5**, 539–548 (1983). doi:10.1016/0191-8141(83)90058-5
113. P. Rochette, L. Sagnotti, G. Consolmagno, L. Folco, A. Maras, F. Panzarino, L. Pesonen, R. Serra, M. Terho, A magnetic susceptibility database for stony meteorites. *Quaderni di Geofisica* **18**, 1–31 (2001).
114. S. J. Morden, The anomalous demagnetization behaviour of chondritic meteorites. *Phys. Earth Planet. Interiors* **71**, 189–204 (1992).
115. J. Gattacceca, P. Rochette, Toward a robust normalized magnetic paleointensity method applied to meteorites. *Earth Planet. Sci. Lett.* **227**, 377–393 (2004). doi:10.1016/j.epsl.2004.09.013
116. E. Jarosewich, R. S. Clarke, Jr., J. N. Barrows, Eds., The Allende meteorite reference sample. *Smithson. Contrib. Earth Sci.* **27**, 1–49 (1986).
117. P. G. Brown, A. R. Hildebrand, M. E. Zolensky, M. Grady, R. N. Clayton, T. K. Mayeda, E. Tagliaferri, R. Spalding, N. D. MacRae, E. L. Hoffman, D. W. Mittlefehldt, J. F. Wacker, J. A. Bird, M. D. Campbell, R. Carpenter, H. Gingerich, M. Glatiotis, E. Greiner, M. J. Mazur, P. J. McCausland, H. Plotkin, T. Rubak Mazur, The fall, recovery, orbit, and composition of the Tagish Lake meteorite: A new type of carbonaceous chondrite. *Science* **290**, 320–325 (2000). doi:10.1126/science.290.5490.320 Medline
118. J. M. Friedrich, M.-S. Wang, M. E. Lipschutz, Comparison of the trace element composition of Tagish Lake with other primitive carbonaceous chondrites. *Meteorit. Planet. Sci.* **37**, 677–686 (2002). doi:10.1111/j.1945-5100.2002.tb00847.x
119. K. Lodders, Solar system abundances and condensation temperatures of the elements. *Astrophys. J.* **591**, 1220–1247 (2003). doi:10.1086/375492
120. Metbase homepage; http://www.metbase.de/home.html (2013).
121. A. Yamakawa, K. Yamashita, A. Makishima, E. Nakamura, Chemical separation and mass spectrometry of Cr, Fe, Ni, Zn, and Cu in terrestrial and extraterrestrial materials using thermal ionization mass spectrometry. *Anal. Chem.* **81**, 9787–9794 (2009). doi:10.1021/ac901762a Medline
122. W. R. Shields, T. J. Murphy, E. J. Catanzaro, E. L. Garner, Absolute isotopic abundance ratios and the atomic weight of a reference sample of chromium. *J. Res. Natl. Bur. Stand.* **70A**, 193–197 (1966). doi:10.6028/jres.070A.016
123. A. Trinquier, J.-L. Birck, C. J. Allègre, C. Göpel, D. Ulfbeck, 53Mn–53Cr systematics of the early solar system revisited. *Geochim. Cosmochim. Acta* **72**, 5146–5163 (2008). doi:10.1016/j.gca.2008.03.023
124. P. H. Warren, Stable-isotopic anomalies and the accretionary assemblage of the Earth and Mars: A subordinate role for carbonaceous chondrites. *Earth Planet. Sci. Lett.* **311**, 93–100 (2011). doi:10.1016/j.epsl.2011.08.047
125. L. Qin, C. M. O. D. Alexander, R. W. Carlson, M. F. Horan, T. Yokoyama, Contributors to chromium isotope variation of meteorites. *Geochim. Cosmochim. Acta* **74**, 1122–1145 (2010). doi:10.1016/j.gca.2009.11.005
126. A. Yamakawa, K. Yamashita, A. Makishima, E. Nakamura, Chromium isotope systematics of achondrites: Chronology and isotopic heterogeneity of the inner solar system bodies. *Astrophys. J.* **720**, 150–154 (2010). doi:10.1088/0004-637X/720/1/150
127. I. Ahn, J. Lee, M. Kusakabe, B. Choi, Oxygen isotope measurements of terrestrial silicates using a CO2-laser BrF5 fluorination technique and the slope of terrestrial fractionation line. *Geosci. J.* **16**, 7–16 (2012). doi:10.1007/s12303-012-0011-x
128. Z. D. Sharp, A laser-based microanalytical method for the in situ determination of oxygen isotope ratios of silicates and oxides. *Geochim. Cosmochim. Acta* **54**, 1353–1357 (1990). doi:10.1016/0016-7037(90)90160-M
129. R. N. Clayton, T. K. Mayeda, Oxygen isotope studies of carbonaceous chondrites. *Geochim. Cosmochim. Acta* **63**, 2089–2104 (1999). doi:10.1016/S0016-7037(99)00090-3
130. E. D. Young, S. S. Russell, Oxygen reservoirs in the early solar nebula inferred from an Allende CAI. *Science* **282**, 452–455 (1998). doi:10.1126/science.282.5388.452
131. R. N. Clayton, T. K. Mayeda, A. E. Rubin, Oxygen isotopic compositions of enstatite chondrites and aubrites. *J. Geophys. Res.* **89**, (S01), C245–C249 (1984). doi:10.1029/JB089iS01p0C245
132. R. N. Clayton, T. K. Mayeda, Oxygen isotope studies of achondrites. *Geochim. Cosmochim. Acta* **60**, 1999–2017 (1996). doi:10.1016/0016-7037(96)00074-9
133. C. Gopel, J.-L. Birck, Mn/Cr systematics: A tool to discriminate the origin of primitive meteorites? Goldschmidt Conference Abstracts, A348 (2010).
134. A. J. Irving, R. Tanaka, A. Steele, S. M. Kuehner, T. E. Bunch, J. H. Wittke, G. M. Hupe, Northwest Africa 6704: A unique cumulate permafic achondrite containing sodic feldspar, awaruite and "fluid" inclusions, with an oxygen isotopic composition in the Acapulcoite-Lodranite field. Annual Meteoritical Society Meeting, #5231 (2011).
135. Q. L. Li, X. H. Li, F. Y. Wu, Q. Z. Yin, H. M. Ye, Y. Liu, G. Q. Tang, C. L. Zhang, In-situ SIMS U-Pb dating of phanerzoic apatite with low U and high common Pb. *Gondwana Res.* **21**, 745–756 (2012). doi:10.1016/j.gr.2011.07.008
136. T. Sano, S. M. Miyama, Magnetorotational instability in protoplanetary disks. I. On the global stability of weakly ionized disks with ohmic dissipiation. *Astrophys. J.* **515**, 776–786 (1999). doi:10.1086/307063
137. J. A. Trotter, S. M. Eggins, Chemical systematics of conodont apatite determined by laser ablation ICPMS. *Chem. Geol.* **233**, 196–216 (2006). doi:10.1016/j.chemgeo.2006.03.004
138. M. Tatsumoto, R. J. Knight, C. J. Allegre, Time differences in the formation of meteorites as determined from the ratio of lead-207 to lead-206. *Science* **180**, 1279–1283 (1973). doi:10.1126/science.180.4092.1279 Medline
139. K. R. Ludwig, User's manual for Isoplot, v. 3.0, a geochronological toolkit for Microsoft Excel. Berkeley Geochronological Center, Special Publication 4 (2003).
140. Y. Amelin, A. Kaltenbach, C. H. Stirling, The U-Pb systematics and cooling rate of plutonic angrite NWA 4590. 42nd Lunar and Planetary Science Conference 2011, Abstract 1682 (2011).
141. T. Mikouchi, K. Sugiyama, W. Satake, Y. Amelin, Mineralogy and Crystallography of Calcium Silico-Phosphate in Northwest Africa 4590 Angrite. 42nd Lunar and Planetary Science Conference 2011, Abstract 2026 (2011).
142. Y. Amelin, A. Ghosh, E. Rotenberg, Unraveling the evolution of chondrite parent asteroids by precise U-Pb dating and thermal modeling. *Geochim. Cosmochim. Acta* **69**, 505–518 (2005). doi:10.1016/j.gca.2004.05.047
143. T. Hiroi, S. Sasaki, S. K. Noble, C. M. Pieters, Space weathering of ordinary chondrite parent bodies, its impact on the method of distinguishing H, L, and LL types and implications for Itokawa samples returned by the Hayabusa mission. 42nd Lunar and Planetary Science Conference 2011, Abstract 1264 (2011).
144. T. Hiroi, M. Abe, K. Kitazato, S. Abe, B. E. Clark, S. Sasaki, M. Ishiguro, O. S. Barnouin-Jha, Developing space weathering on the asteroid 25143 Itokawa. *Nature* **443**, 56–58 (2006). doi:10.1038/nature05073 Medline

145. R. H. Biswas, P. Morthekai, R. K. Gartia, S. Chawla, A. K. Singhvi, Thermoluminescence of the meteorite interior: A possible tool for the estimation of cosmic ray exposure ages. *Earth Planet. Sci. Lett.* **304**, 36–44 (2011). doi:10.1016/j.epsl.2011.01.012
146. D. W. G. Sears, A. A. Mills, Temperature gradients and atmospheric ablation rates for the Barwell meteorite. *Nat. Phys. Sci (Lond.)* **242**, 25–26 (1973). doi:10.1038/physci242025a0
147. R. Chen, S. W. S. McKeever, Theory of thermoluminescence and related phenomena. (World Scientific, Singapore, 1997), 560 pp.
148. D. W. G. Sears, K. Ninagawa, A. Signhvi, Luminescence studies of extraterrestrial materials: Insights into their recent radiation and thermal histories and into their metamorphic history. *Chemie Erde Geochemistry* **73**, 1–37 (2013). http://dx.doi.org/10.1016/j.chemer.2012.12.001
149. M. Haq, F. A. Hasan, D. W. G. Sears, Thermoluminescence and the shock and reheating history of meteorites- IV: The induced TL properties of type 4-6 ordinary chondrites. *Geochim. Cosmochim. Acta* **52**, 1679–1689 (1988). doi:10.1016/0016-7037(88)90236-0
150. R. K. Guimon, K. S. Weeks, B. D. Keck, D. W. G. Sears, Thermoluminescence as a palaeothermometer. *Nature* **311**, 363–365 (1984). doi:10.1038/311363a0
151. W. R. Van Schmus, J. A. Wood, A chemical-petrologic classification for the chondritic meteorites. *Geochim. Cosmochim. Acta* **31**, 747–765 (1967). doi:10.1016/S0016-7037(67)80030-9
152. D. W. G. Sears, J. N. Grossman, C. L. Melcher, L. M. Ross, A. A. Mills, Measuring the metamorphic history of unequilibrated ordinary chondrites. *Nature* **287**, 791–795 (1980). doi:10.1038/287791a0
153. C. P. Hartmetz, R. Ostertag, D. W. G. Sears, A thermoluminescence study of experimentally shock-loaded oligoclase and bytownite. *J. Geophys. Res.* **91**, (B13), E263–E274 (1986). doi:10.1029/JB091iB13p0E263
154. P. H. Benoit, H. Sears, D. W. G. Sears, The natural thermoluminescence of meteorites- IV: Ordinary chondrites at the Lewis Cliff ice field. *J. Geophys. Res.* **97**, (B4), 4629–4647 (1992). doi:10.1029/91JB02982
155. P. Schmitt-Kopplin, Z. Gabelica, R. D. Gougeon, A. Fekete, B. Kanawati, M. Harir, I. Gebefuegi, G. Eckel, N. Hertkorn, High molecular diversity of extraterrestrial organic matter in Murchison meteorite revealed 40 years after its fall. *Proc. Natl. Acad. Sci. U.S.A.* **107**, 2763–2768 (2010). doi:10.1073/pnas.0912157107 Medline
156. D. Tziotis, N. Hertkorn, P. Schmitt-Kopplin, Kendrick-analogous network visualisation of ion cyclotron resonance Fourier transform mass spectra: Improved options for the assignment of elemental compositions and the classification of organic molecular complexity. *Eur. J. Mass Spectrom. (Chichester, Eng.)* **17**, 415–421 (2011). doi:10.1255/ejms.1135 Medline
157. C. M. Hohenberg, F. A. Podosek, J. R. Shirck, K. Arti, R. C. Reedy, Comparisons between observed and predicted cosmogenic noble gases in lunar samples. In: Proceedings 9th Lunar and Planetary Science Conference, Houston, TX, March 13–17, 1978, Vol. 2, New York, Pergamon Press, Inc., pp. 2311–2344 (1978).

Acknowledgments: The Russian Academy of Sciences field study of the Chelyabinsk airburst was supported by the Institute for Dynamics of Geospheres and grants of the Federal Targeted Program "Scientific and Educational Human Resources of Innovation-Driven Russia" and the RAS Presidium Program "Fundamental Problems of Investigation and Exploration of the Solar System". The office of Chelyabinsk Oblast Governor Mikhail Yurevich provided assistance. S. Petukhov and I. Talyukin from the Universe History Museum in Dedovsk contributed samples, as did M. Boslough of Sandia National Laboratories. U. Johann (Astrium Satellites GmbH) calculated the Chebarkul hole position from Pléiades 1A satellite observations. D. F. Blake provided use of a petrographic microscope. P.J. acknowledges support from the NASA Near Earth Object Observation Program, Q.Z.Y. and M.E.Z. from the NASA Cosmochemistry Program, and M.G. by the Academy of Finland.

Supplementary Materials
www.sciencemag.org/cgi/content/full/science.1242642/DC1
Supplementary Text
Figs. S1 to S87
Tables S1 to S24
References (*42–157*)

1 July 2013; accepted 28 October 2013
Published online 7 November 2013
10.1126/science.1242642

Author Affiliations
[1]Institute for Dynamics of Geospheres of the Russian Academy of Sciences, Leninsky Prospect 38, Building 1, Moscow, 119334, Russia. [2]SETI Institute, 189 Bernardo Ave, Mountain View, CA 94043, USA. [3]NASA Ames Research Center, Moffett Field, Mail Stop 245-1, CA 94035, USA. [4]Institute of Astronomy of the Russian Academy of Sciences, Pyatnitskaya 48, Moscow, 119017, Russia. [5]Department of Theoretical Mechanics, South Ural State University, Lenin Avenue 76, Chelyabinsk, 454080, Russia. [6]Chelyabinsk State University, Bratyev Kashirinyh Street 129, Chelyabinsk, 454001, Russia. [7]Institute of Physics and Technology, Ural Federal University, Mira Street 19, Yekaterinburg, 620002, Russia. [8]Vernadsky Institute of Geochemistry and Analytical Chemistry of the RAS, Kosygina Street 19, Moscow, 119991, Russia. [9]Department of Earth and Planetary Sciences, University of California at Davis, Davis, CA 95616, USA. [10]Department of Physics, University of Helsinki, P. O. Box 64, 00014 Helsinki, Finland. [11]Koninklijk Nederlands Meteorologisch Instituut, P. O. Box 201, 3730 AE De Bilt, Netherlands. [12]Department of Geoscience and Engineering, Faculty of Civil Engineering and Geosciences, Delft University of Technology, P.O. Box 5048, 2600 GA Delft, Netherlands. [13]Tomsk State University, Lenina Prospect 36, Tomsk, 634050 Russia. [14]Research and Production Association "Typhoon", fl. 2, 7 Engels Street, Obninsk, 249032, Russia. [15]Support Foundation for Astronomy "Ka-Dar", P.O. Box 82, Razvilka, 142717 Russia. [16]Science and Technology Center of the Social and Youth Initiatives Organization, 3-12-63 Udal'tsova Street, Moscow, 119415, Russia. [17]University of Oslo, Physics Building, Sem Saelands Vel 24, 0316 Oslo, Norway. [18]Institute of Engineering Sciences Urals Branch of the Russian Academy of Sciences, Komsomolskaya Street 34, Yekaterinburg, 620049, Russia. [19]Center for Molecular and Genomic Imaging, University of California, Davis, Davis, CA 95616, USA. [20]Department of Earth and Planetary Sciences, American Museum of Natural History, New York, NY 10024, USA. [21]Department of Chemistry, Fordham University, Bronx, NY 10458, USA. [22]Astromaterials Research and Exploration Science, NASA Johnson Space Center, Houston, TX 77058, USA. [23]Jacobs Technology, 2224 Bay Area Boulevard, Houston TX 77058, USA. [24]Institute of Meteoritics, University of New Mexico, Albuquerque, NM 87131–0001, USA. [25]Department of Earth and Planetary Materials Science, Tohoku University, Aramaki, Aoba, Sendai, Miyagi 980-8578, Japan. [26]Division of Polar Earth-System Sciences, Korea Polar Research Institute, 26 Songdomi rae, Yeonsu-gu, Incheon 406-840, Korea. [27]National Astronomical Observatories, Beijing, Chinese Academy of Sciences, Beijing 100012, China. [28]State Key Laboratory of Lithospheric Evolution, Institute of Geology and Geophysics, Chinese Academy of Sciences, Beijing 100029, China. [29]Department of Geological Sciences, Brown University, Providence, RI 02912, USA. [30]Analytical BioGeoChemistry, Helmoltz Zentrum Muenchen, Ingoldstäter Landstrasse 1, D-85764 Obeschleissheim, Germany. [31]Technical University Muenchen, Analytical Food Chemistry, Alte Akademie 10, 85354 Freising, Germany. [32]Geochemical Research Center, The University of Tokyo, 7-3-1 Hongo, Bunkyo-ku, Tokyo 113-0033, Japan. [33]Waseda Institute for Advanced Study, Waseda University, 1-6-1 Nishiwaseda, Shinjuku, Tokyo 169-8050, Japan. [34]Department of Earth and Planetary Science, The University of Tokyo, 7-3-1 Hongo, Bunkyo-ku, Tokyo 113-0033, Japan.

Table 1. Atmospheric trajectory and pre-atmospheric orbit for the Chelyabinsk meteoroid, with 2 standard deviation uncertainties. Angular elements are for equinox J2000.0.

Atmospheric trajectory	Chelyabinsk	Pre-atmospheric orbit	Chelyabinsk	Itokawa
H_b (beginning height, km)	97.1 ± 1.6	T_J (Tisserand's parameter)	3.87 ± 0.24	4.90
H_m (peak brightness, km)	29.7 ± 1.4	a (semimajor axis, AU)	1.76 ± 0.16	1.324
H_f (disruption, km)	27.0 ± 1.4	e (eccentricity)	0.581 ± 0.018	0.280
H_e (end height, km)	13.6 ± 1.4	q (perihelion distance, AU)	0.739 ± 0.020	0.953
V_∞ (entry speed, km/s)	19.16 ± 0.30	ω (argument of perihelion, °)	108.3 ± 3.8	162.8
h (entry elevation angle, °)	18.3 ± 0.4	Ω (longitude of ascending node, °)	326.4422 ± 0.0028	69.1
a_z (entry azimuth angle from South, °)	283.2 ± 0.4	i (inclination, °)	4.93 ± 0.48	1.6
V_g (geocentric entry speed, km/s)	15.3 ± 0.4	Q (aphelion distance, AU)	2.78 ± 0.20	1.70
Ra_g (geocentric right ascension of radiant, °)	333.2 ± 1.6	T_p (perihelion time)	2012-12-31.9 ± 2.0	2013-07-10.8
Dec_g (geocentric declination of radiant, °)	+0.3 ± 1.8	Epoch (ET)	2013-02-15.139	2013-04-18.0

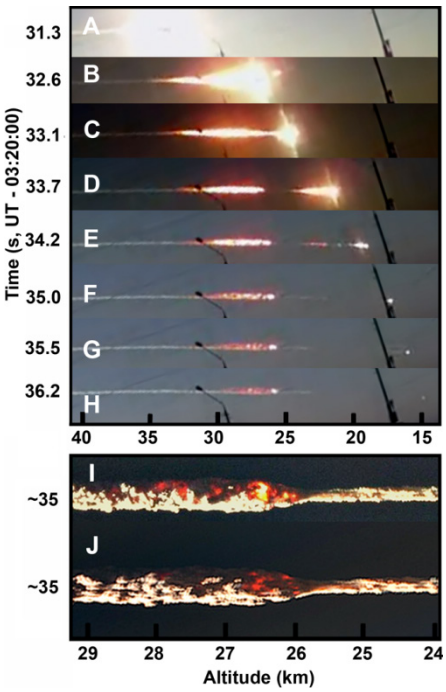

Fig. 1. Meteoroid fragmentation stages in video taken by Aleksandr Ivanov in Kamensk-Uralskiy. (**A**) Fireball just before peak brightness, at the moment when camera gain first adjusted. (**B**) End of main disruption. (**C**) Onset of secondary disruption. (**D**) End of secondary disruption, main debris cloud continues to move down. (**E**) Two main fragments remain. (**F**) Single fragment remains. (**G**) Thermally emitting debris cloud at rest with atmosphere. (**H**) Final fragment continues to penetrate. Meteor moved behind distant lamp posts. (**I** and **J**) Detail of the thermal emission from a photograph by Mr. Dudarev (I) and Marat Ahmatvaleev (J), after sky subtraction with high-pass filter and contrast enhancement. Altitude scale is uncertain by ±0.7 km.

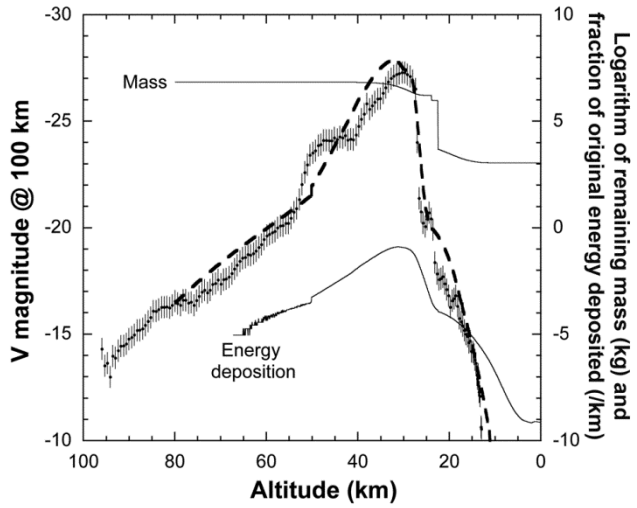

Fig. 2. Fireball visual magnitude irradiance lightcurve, normalized to 100 km distance. The bold dashed line shows the model fit to the lightcurve (SM Sect. 1.2), with thin lines showing total mass of all fragments passing a given altitude (kg) and the altitude dependent rate of energy deposition as a fraction of the original kinetic energy (km^{-1}).

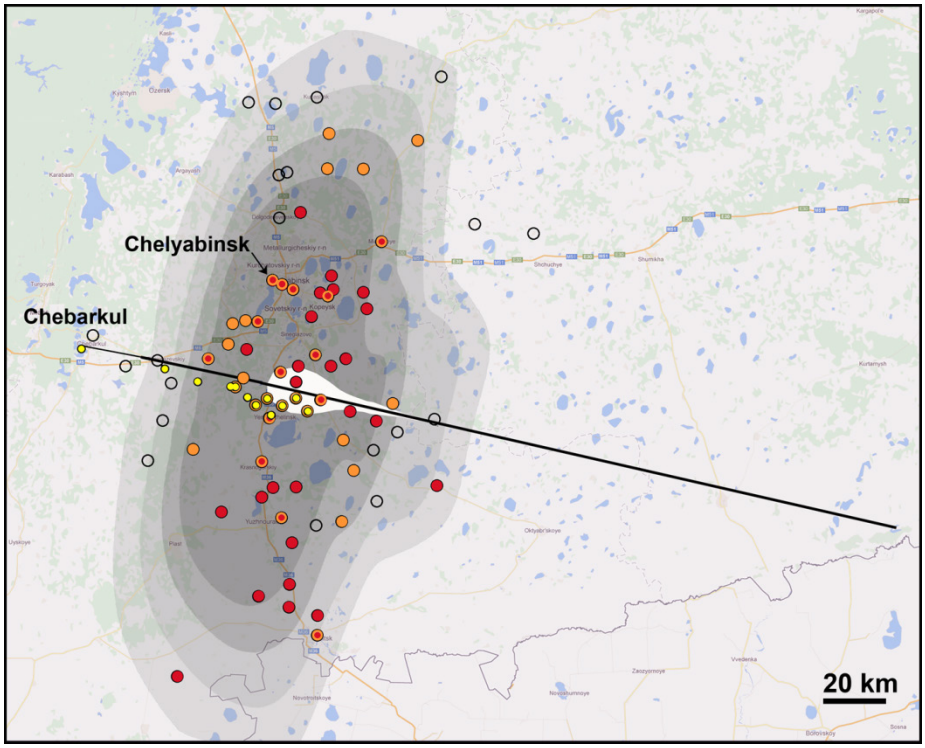

Fig. 3. Map of glass damage on the ground with models of overpressure. Field survey data are shown in solid orange circles for reported damage and open black circles for no damage, while solid red circles are the most damaged villages in each district reported by the government. Each point, irrespective of population density, represents one of many villages or city districts scattered throughout the area. Model contours (with progressive grey scale) represent kinetic energies and over pressures from inside out: 300 kT $\Delta p > 1{,}000$ Pa, 520 kT $\Delta p > 1{,}000$ Pa, 300 kT $\Delta p > 500$ Pa, and 520 kT $\Delta p > 500$ Pa, respectively. Also shown are the locations of meteorite finds (yellow points) and the ground-projected fireball trajectory (black line), moving from 97 km altitude right to 14 km altitude left. White shows the fireball brightness on a linear scale.

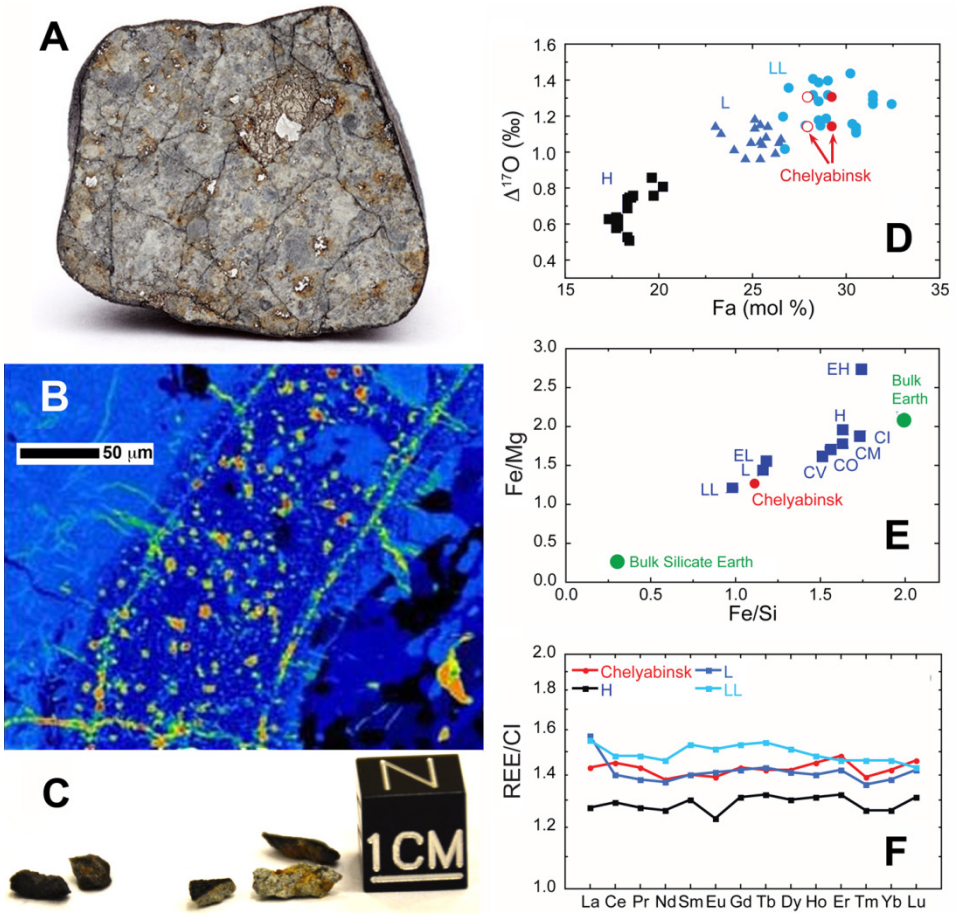

Fig. 4. Meteorite material properties, chemical and isotopic compositions. (**A**) Chelyabinsk meteorite (diameter ~4 cm) showing shock veins. (**B**) Fe element map of a shock vein. Note the metal layer (shown in green) located ~20 microns inside the vein. (**C**) Meteorite fragments recovered from the ice covered lake Chebarkul. (**D**) $\Delta^{17}O$ versus Fa mol% of olivine in Chelyabinsk, compared to other ordinary chondrites of type H, L, and LL (*38*). Fa is defined as mole ratio of Fe/(Fe+Mg) in olivine. Average $\Delta^{17}O$ values from UNM (1.15 ± 0.06‰) and from KOPRI (1.31 ± 0.04‰) for Chelyabinsk likely reflect indigenous heterogeneity in oxygen isotopes. Solid symbols are Fa number measured in this study (SM Sect. S4.3), while open symbols are from (*18*). (**E**) Ratio plots of the three major elements (Mg, Si, Fe; together with oxygen >90% of mass) for Chelyabinsk and the main chondrite groups. The bulk Earth and bulk silicate Earth compositions were taken from (*39*), chondrite compositions from (*40*). (**F**) CI chondrite normalized rare earth elemental pattern of Chelyabinsk compared to the average chondrite group compositions of (*38*, *41*).